COMMUNICATION

Field Emission of Single-Layer Graphene Films Prepared by Electrophoretic Deposition

By *Zhong-Shuai Wu, Songfeng Pei, Wencai Ren,* Daiming Tang, Libo Gao, Bilu Liu, Feng Li, Chang Liu,* and *Hui-Ming Cheng**

Since the first demonstration of the electron field emission of carbon nanotubes (CNTs),[1] various low-dimensional carbon materials, including nanotubes,[1–6] nanofibers,[7] nanohelices,[8] nanotips,[9] nanorods,[10] nanocones,[11] and nanowalls[12] have been extensively studied to explore their applications as electron sources because of their unique structure, and excellent electronic and mechanical properties. Especially, CNTs demonstrate promising electron-field-emission properties far superior to the conventional field emitters: low turn-on voltage and high emission current.

Graphene,[13–15] two-dimensional graphite, as a rising star in material science, shares many similar or even identical properties as CNTs. It has atomic thickness, high aspect ratio (the ratio of lateral size to thickness), excellent electrical conductivity, and good mechanical properties, which qualify it as an attractive candidate for the use of field emission source. Furthermore, the presence of rich edges may render graphene superior to CNTs for the tunneling of electrons. Previous studies have demonstrated that thin carbon nanoflakes/nanosheets prepared by plasma-enhanced chemical vapor deposition (PEVCD)[16–21] show promising electron-emission properties, such as low emission threshold field and large emission current density. However, the field-emission properties of single-layer graphene have not been studied, due to the difficulties on both large-scale synthesis of graphene and fabrication of field-emission cathode. Recent progress on the large-scale synthesis of single-layer graphene by chemical exfoliation[22–26] opens up the possibility to investigating their field-emission properties, although assembly of graphene into continuous or patterned films is required for the given utilization of graphene in practical flat-panel displays.

Electrophoretic deposition (EPD) is an economical and versatile processing technique that has been applied in deposition of coatings and films, as for example phosphors for display.[27] It has many advantages in the preparation of thin films from suspensions, such as high deposition rate and throughput, good uniformity and controlled thickness of the obtained films, no need of binders, and simplicity of scaling up. For example, Gao et al.[28] fabricated CNT films with good microstructural homogeneity and high packing density from colloidal CNT suspensions utilizing this technique, which showed excellent electron-field-emission characteristics. By combining EPD with the fissure-formation technique, Jung et al.[29] obtained horizontally aligned CNT field emitters strongly adhered to the substrate and having significantly enhanced field-emission properties.

Here, we report the fabrication and field-emission properties of single-layer graphene films by EPD from a stable suspension of isopropyl-alcohol-dispersed graphene prepared by chemical exfoliation. The graphene films display good field-emission properties with low turn-on electric field and threshold field, large field-enhancement factor, and good emission stability and uniformity, which are much better than those of its graphene-powder counterpart and well comparable or even better than those of CNTs.

The graphene used in this study was prepared by chemical exfoliation of artificial graphite (particle size $\leq 30\,\mu m$), as we reported elsewhere.[30] Atomic force microscopy (AFM) and transmission electron microscopy (TEM) measurements (Fig. 1) indicate that the as-prepared graphene sheets (≤ 3 layers) have a relatively smooth and planar structure (Fig. 1a), similar to that obtained by micromechanical cleavage,[13] and consist of up to 80% single-layer graphene.[30] Notably, the single-layer graphene has a high aspect ratio, with a thickness of ~ 1.1 nm (Fig. 1a) and a lateral size on the order of micrometers (Fig. 1). More importantly, the sheets exhibit a high electrical conductivity of $\sim 1 \times 10^3\,S\,cm^{-1}$,[30] indicating their high quality and ensuring their promising applications as conductive materials and in electronic devices.

Essentially, the EPD technique includes two key steps.[31] First, charged colloidal particles in a liquid-phase suspension are forced to move toward the oppositely charged electrode under an electric field. Second, these charged particles are coherently deposited onto the surface of an electrically conductive electrode. To obtain a stable graphene suspension, the prerequisite for EPD, the graphene obtained was first dispersed in isopropyl alcohol by sonication for 1 h. The obtained suspension was stable enough for EPD because of the presence of residual polar oxygen-containing groups on the graphene sheets. $Mg(NO_3)_2 \cdot 6H_2O$ as charger was then added, to render the graphene sheets positively charged. The weight ratio of graphene to $Mg(NO_3)_2 \cdot 6H_2O$ was controlled to 1:1. After these treatments, a uniform and stable suspension of Mg^{2+}-absorbed graphene sheets was obtained, as shown in Figure 2a.

Figure 2b is a diagram of the EPD process used to prepare graphene films. A stainless steel substrate was used as positive electrode, and indium tin oxide (ITO)-coated conductive glass as

[*] Prof. H.-M. Cheng, Dr. W. C. Ren, Z.-S. Wu, S. F. Pei, D. M. Tang, L. B. Gao, B. L. Liu, Dr. F. Li, Dr. C. Liu
Shenyang National Laboratory for Materials Science
Institute of Metal Research
Chinese Academy of Sciences
72 Wenhua Road, Shenyang 110016 (P. R. China)
E-mail: cheng@imr.ac.cn; wcren@imr.ac.cn

DOI: 10.1002/adma.200802560

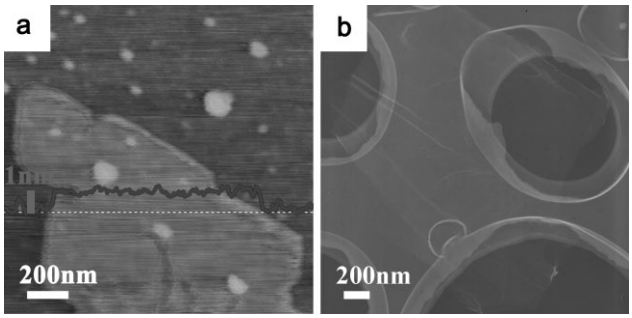

Figure 1. a) Tapping-mode AFM image of a graphene sheet showing a flat structure. Inset: the corresponding height profile of the graphene, revealing the average thickness of ~1.1 nm. b) TEM image of a graphene film, displaying a smooth and flat structure with a few folds.

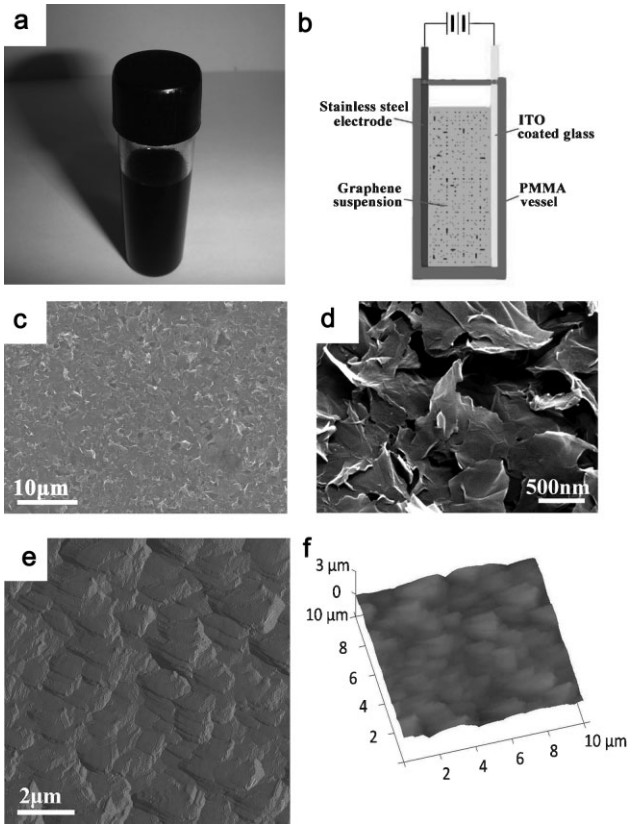

Figure 2. a) Optical image of the stable graphene suspension (0.2 mg mL^{-1}) used for EPD. b) Diagram of the EPD process used to prepare graphene films. c) Low-magnification and d) high-magnification SEM images of the graphene film deposited on the ITO-coated glass for 1 min at an applied field of 160 V by EPD, using a ~0.1 mg mL^{-1} graphene suspension as electrolyte. e) Tapping-mode AFM amplitude image (10 μm × 10 μm) and f) the corresponding 3D surface plot of the graphene film fabricated by EPD.

negative electrode. The Mg^{2+}-absorbed graphene suspension was loaded in a polymethylmethacrylate (PMMA) vessel as the electrolyte. The distance between the two electrodes was 5 mm, and the applied voltage was 100–160 V. Under the applied voltage, the positively charged graphene sheets migrated toward the negative electrode, and were subsequently orderly deposited onto the surface of the negative electrode. The thickness of the graphene films could be tuned ranging from several nanometers to a few micrometers by varying the deposition conditions, including the concentration of graphene and Mg^{2+} ions in the electrolyte, the applied voltage, and the deposition time. We consider that the migration and subsequent deposition of graphene under the applied voltage are subject to the preferential absorption of Mg^{2+} ions by graphene sheets in isopropyl alcohol solution, similar to the preferential absorption of Mg^{2+} ions on the suspended CNTs.[28] Additionally, it is worth noting that the presence of Mg^{2+} salt also plays an important role in improving the adhesion of graphene to the substrates, and in determining the deposition rate during the EPD process.

Figure 2c shows a typical low-magnification scanning electron microscopy (SEM) image of the graphene film obtained after 1 min of deposition on ITO-coated glass. It can be found that the film has a high graphene density and uniform morphology. A high-magnification SEM image (Fig. 2d) indicates that the graphenes are randomly oriented, and some of them are almost normal to the substrate due to their good stiffness, exhibiting numerous sharp edges. These sharp edges will act as active emission sites to enhance the electron field emission. AFM was also used to further elucidate the detailed structure of graphene in the films. The amplitude image of the graphene film shown in Figure 2e provides clear evidence of the presence of a great deal of graphene edges on the film surface. Moreover, these graphenes are not aggregated, but separated with a varying distance ranging from several to hundreds of nanometers. The 3D surface plot in Figure 2f reveals that the surface roughness of the graphene film is up to ~200 nm. This suggests that the graphene in the films retains its intrinsic high aspect ratio. These structural characteristics make graphene films ideal candidates for field emitters.

For comparison, we also fabricated graphene-based field emitters by directly coating graphene powder on a conductive tape. Figure 3a shows the low-magnification SEM image of graphene-powder coating. It is clearly seen that the individual graphene tends to aggregate into sparsely distributed large particles with a sizes up to 10 μm. Moreover, it is worth noting that the density of graphene is much lower than that of the films prepared by EPD. The higher-magnification SEM image in Figure 3b reveals that most of the individual graphene sheets are seriously overlapped and aggregated with a direction nearly parallel to the surface, and only a few protruding sharp edges normal to the surface were found. Therefore, less-active emission tips exist in the same area for the graphene-powder coating than for the graphene film.

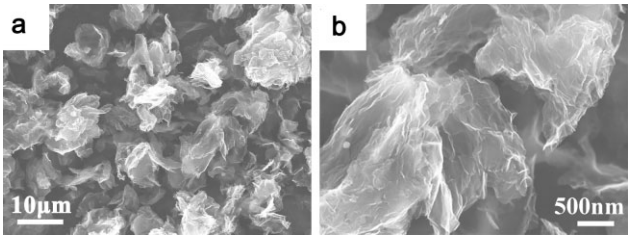

Figure 3. a) Low-magnification and b) high-magnification SEM images of the graphene-powder coating on a conductive tape.

The electron-field-emission characteristics of the graphene films and graphene-powder coating were measured in a ball-type chamber with a vacuum of 10^{-5} Pa. The anode was a cylinder-shaped iron probe with a diameter of 1 mm, and the graphene film or graphene-powder coating was fixed onto a copper stage with conductive glue as the cathode. In the measurements, the interelectrode distance remains 100 μm. The current–voltage (I–V) characteristics were investigated by a custom-made diode I–V measurement system, in which the bias was supplied by a power source (Keithley 248).[32] Figure 4a shows the current density (J) of the graphene film and graphene-powder coating as a function of applied electric field (E). The turn-on electric field (E_{to}, 2.3 V μm^{-1} at 10 μA cm^{-2}) and the threshold field (E_{thr}, 5.2 V μm^{-1} at 10 mA cm^{-2}) of the graphene films are substantially lower than those of the graphene-powder coating (E_{to}, 5.2 V μm^{-1}, E_{thr}, 9.6 V μm^{-1}). We suggest that this is attributed to the higher density of effective emission tips in the film, that is, the edges of vertically oriented graphene, as shown in Figure 2c–f. Moreover, it is worth noting that the E_{to} value of graphene films is significantly lower than those from Spindt-type Mo emitters[33] and wide-band-gap semiconducting materials,[6,34–39] such as nanostructured diamond films, AlN, and LiF. The E_{to} value of graphene films is also lower than that of free-standing sub-nanometer graphite sheets (E_{to}, 4.7 V μm^{-1}) synthesized by PECVD,[19] and the E_{to} and E_{thr} values are well comparable to those of CNT films fabricated by EPD (E_{to}, 1.4–3.0 V μm^{-1})[28,29,40,41] and screen-printing (E_{to}, 2–6.4 V μm^{-1}) techniques.[42]

The Fowler–Nordheim (F–N) theory is the most-commonly used model for understanding the electron emission from a metal surface under a strong applied field, and it has been also widely used to investigate the electron-emission behavior of various nanostructures, such as CNTs,[3–5,43–45] nanowires,[46] and nanowalls.[47] To elucidate the electron-emission mechanism and the differences in the field-emission behaviors of graphene-powder coating and graphene film, we plotted ln (J/E^2) versus $1/E$, which yields a line, in good agreement with the F–N equation (Fig. 4b). This agreement confirms that the current is indeed the result of field emission. Because of the sharp edges with atomic thickness and high aspect ratio, a dramatically enhanced local electric field at the emitting surface of graphene film is expected compared with the applied electric field. Assuming that the work function of graphene is the same as that of graphite (~5 eV), the field-enhancement factor (β) of a graphene film was determined to be ~3700 from the constant F–N slope in the low-current region, which is significantly higher than that of graphene powder (~800). This large enhancement factor allows for sufficient tunneling of electrons from graphene through barriers, which results in the low turn-on and threshold voltages, as shown above.

To evaluate the field-emission stability of single-layer graphene films, we monitored the current density over 12 h with the starting current densities of 2.23, 6.36, and 11.46 mA cm^{-2}, as shown in Figure 4c. It can be found that the graphene film exhibits excellent emission stability without degradation at lower current density (2.23 mA cm^{-2}). Under large applied electric fields, the current density shows a slight increase at the beginning, and then becomes stable with a small degradation of ~2 and ~4% for the starting current densities of 6.36 and

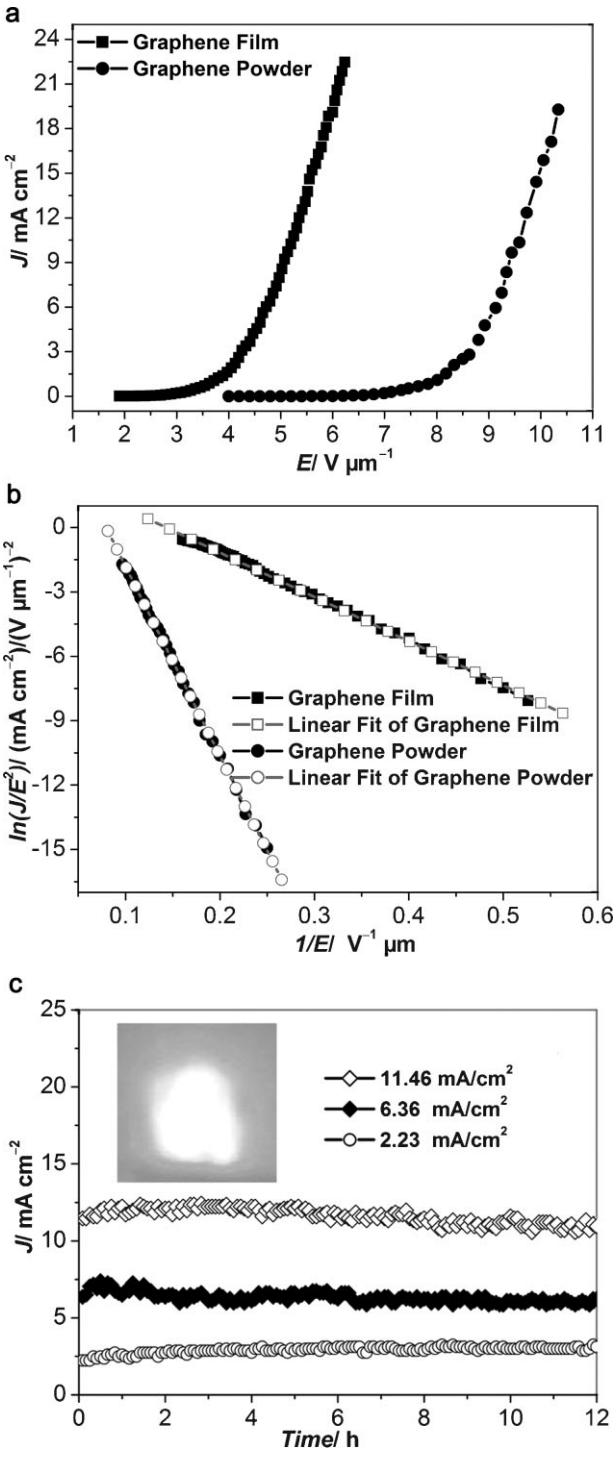

Figure 4. a) Typical plots of the electron-emission current density (J) as a function of applied electric field (E) for the graphene film and graphene-powder coating. b) Corresponding F–N plots. c) Emission stability of the graphene film prepared by EPD at different constant electric fields and a vacuum of 10^{-5} Pa at room temperature within 12 h. Inset: emission pattern for the graphene-film emitter with a size of ~1 cm × 1 cm, which was collected at an applied field of 3.8 V μm^{-1}.

11.46 mA cm^{-2}, respectively. It should be emphasized here that, for a similar current density, our single-layer graphene film exhibits much better emission stability than single-walled-CNT (SWCNT) and multiwalled-CNT (MWCNT) films fabricated using the spray method,[48] EPD, or combination of EPD and other techniques,[29,41] and grown by the CVD process.[28] Previous studies[4] showed that the emission degradation is a factor of 10 faster for SWCNTs than for MWCNTs, because of the single shells of SWCNTs are more sensitive to ion bombardment and irradiation, while the multiple shells of MWCNTs tend to stabilize their structure. Considering the fact that the graphene has unpaired edge atoms, they are also very susceptible to ion bombardment and irradiation, similar to the SWCNTs. Therefore, we consider that the excellent stability of our graphene emitter may be attributed to the homogeneous surface morphology of the graphene films, as shown in Figure 2c–f. In the case of CNTs, due to the high aspect ratio the surface morphology of the cathode results in some protruding CNT emitters involved in field emission, and these emitters are suffering from the excessive emission, leading to disintegration of emitter.[48,49] However, in the case of graphene the current is expected to be shared with atoms on line edges. Therefore, the homogeneity of graphene films is probably responsible for their excellent emission stability. Additionally, because graphene has a large lateral size and good flexibility, it is reasonable to expect that the randomly oriented graphene sheets may be aligned to the electron-field direction under an applied field. Therefore, we think that the initial increase of emission current may be caused by the increase of the effective field-emission tips on the film surface. We also measured the emission pattern from the graphene-film emitter using a phosphor-coated ITO glass. A uniform emission pattern with a total emission current of 0.58 mA was obtained under an applied field of 3.8 V μm^{-1}, revealing the emission uniformity (Inset of Fig. 4c). Combining the low E_{to} and E_{thr}, high enhancement factor, good stability, and emission uniformity, we expect that the graphene films fabricated by EPD have great potential, and are good candidates for next-generation field emitters.

The excellent field-emission properties of graphene films can be ascribed to the following aspects. Intrinsically, graphene has an atomic thickness, high aspect ratio, excellent electrical conductivity, and good mechanical properties, which satisfy all the requirements for a good field emitter. Consequently, a remarkably enhanced local electric field and good electron-emission stability can be expected for this material. Furthermore, the atoms at graphene edges may form a distorted sp^3-hybridized geometry instead of a planar sp^2-hybridized configuration. As a result, there should be localized states at graphene edges, and possible barriers to the electron emission are decreased. Therefore, we consider that the presence of graphene edges is another key factor responsible for the excellent field-emission properties. These results are very similar to those previously reported for CNTs, where opened CNTs exhibit better field emission properties than closed ones.[4] Third, the graphene film fabricated by EPD has a uniform morphology and high graphene density, and some graphene edges are nearly normal to the substrate. This ensures emission uniformity and sufficient effective field-emission tips on the film surface. Fourth, both the interface contact and adhesion between graphene film and the substrate are good due to the formation of metal hydroxide from the metal ions at the electrode surface during the EPD process.[28] This good adhesion and contact facilitates electron transport, and consequently improves the field emission performance. We believe that the field emission properties of graphene films can be further improved by optimizing the intrinsic structure of graphenes, the EPD processing, and the morphology and thickness of the films.

In summary, we applied the EPD technique to fabricate homogeneous single-layer graphene films, and investigated the field-emission properties of these films. The graphene films have high density, uniform thickness, numerous edges normal to the film surface, and good interface contact and adhesion with the substrate, which ensure the full utilization of the unique structure and excellent properties of graphenes. The single-layer graphene films show excellent field-emission properties, with $E_{to} = 2.3$ V μm^{-1}, $E_{thr} = 5.2$ V μm^{-1}, a large field-enhancement factor of ~3700, and good emission stability and uniformity, which are much better than those of a graphene-powder coating and well comparable or even better to those of CNTs. The above results suggest that single-layer graphenes have a great potential as high-performance field emitters.

Acknowledgements

This work was supported by Ministry of Science and Technology of China (no. 2006CB932703), National Science Foundation of China (no. 90606008), Chinese Academy of Sciences (no. KJCX2-YW-M01), and the Knowledge Innovation Program of CAS. The authors acknowledge Dr. K. L. Jiang and Z. Chen for the kind help on the emission pattern measurements.

Received: August 31, 2008
Revised: December 5, 2008
Published online: February 25, 2009

[1] W. A. Deheer, A. Chatelain, D. Ugarte, *Science* **1995**, *270*, 1179.
[2] S. S. Fan, M. G. Chapline, N. R. Franklin, T. W. Tombler, A. M. Cassell, H. J. Dai, *Science* **1999**, *283*, 512.
[3] J. M. Bonard, J. P. Salvetat, T. Stockli, L. Forro, A. Chatelain, *Appl. Phys. A Mater. Sci. Proc.* **1999**, *69*, 245.
[4] J. M. Bonard, H. Kind, T. Stockli, L. A. Nilsson, *Solid-State Electr.* **2001**, *45*, 893.
[5] Y. Cheng, O. Zhou, *C. R. Phys.* **2003**, *4*, 1021.
[6] S. C. Lim, K. Lee, I. H. Lee, Y. H. Lee, *Nano* **2007**, *2*, 69.
[7] C. H. Weng, K. C. Leou, H. W. Wei, Z. Y. Juang, M. T. Wei, C. H. Tung, C. H. Tsai, *Appl. Phys. Lett.* **2004**, *85*, 4732.
[8] G. Y. Zhang, X. Jiang, E. G. Wang, *Appl. Phys. Lett.* **2004**, *84*, 2646.
[9] C. L. Tsai, C. F. Chen, L. K. Wu, *Appl. Phys. Lett.* **2002**, *81*, 721.
[10] R. Che, M. Takeguchi, M. Shimojo, K. Furuya, *J. Phys: Conf. Ser.* **2007**, *61*, 200.
[11] L. R. Baylor, V. I. Merkulov, E. D. Ellis, M. A. Guillorn, D. H. Lowndes, A. V. Melechko, M. L. Simpson, J. H. Whealton, *J. Appl. Phys.* **2002**, *91*, 4602.
[12] Y. H. Wu, B. J. Yang, B. Y. Zong, H. Sun, Z. X. Shen, Y. P. Feng, *J. Mater. Chem.* **2004**, *14*, 469.
[13] K. S. Novoselov, A. K. Geim, S. V. Morozov, D. Jiang, Y. Zhang, S. V. Dubonos, I. V. Grigorieva, A. A. Firsov, *Science* **2004**, *306*, 666.
[14] A. K. Geim, K. S. Novoselov, *Nat. Mater.* **2007**, *6*, 183.
[15] Y. Kopelevich, P. Esquinazi, *Adv. Mater.* **2007**, *19*, 4559.
[16] N. G. Shang, C. P. Li, W. K. Wong, C. S. Lee, I. Bello, S. T. Lee, *Appl. Phys. Lett.* **2002**, *81*, 5024.

[17] A. N. Obraztsov, A. P. Volkov, A. A. Zakhidov, D. A. Lyashenko, Y. V. Petrushenko, O. P. Satanovskaya, *Appl. Surf. Sci.* **2003**, *215*, 214.
[18] J. J. Wang, M. Y. Zhu, X. Zhao, R. A. Outlaw, D. M. Manos, B. C. Holloway, C. Park, T. Anderson, V. P. Mammana, *J. Vac. Sci. Technol. B* **2004**, *22*, 1269.
[19] J. J. Wang, M. Y. Zhu, R. A. Outlaw, X. Zhao, D. M. Manos, B. C. Holloway, V. P. Mammana, *Appl. Phys. Lett.* **2004**, *85*, 1265.
[20] S. K. Srivastava, A. K. Shukla, V. Vankar, V. Kumar, *Thin Solid Films* **2005**, *492*, 124.
[21] M. Y. Chen, C. M. Yeh, J. S. Syu, J. Hwang, C. S. Kou, *Nano* **2007**, *18*, 185706.
[22] S. Stankovich, D. A. Dikin, R. D. Piner, K. A. Kohlhaas, A. Kleinhammes, Y. Jia, Y. Wu, S. T. Nguyen, R. S. Ruoff, *Carbon* **2007**, *45*, 1558.
[23] H. C. Schniepp, J. L. Li, M. J. McAllister, H. Sai, M. Herrera-Alonso, D. H. Adamson, R. K. Prud'homme, R. Car, D. A. Saville, I. A. Aksay, *J. Phys. Chem. B* **2006**, *110*, 8535.
[24] S. Niyogi, E. Bekyarova, M. E. Itkis, J. L. McWilliams, M. A. Hamon, R. C. Haddon, *J. Am. Chem. Soc.* **2006**, *128*, 7720.
[25] S. Gilje, S. Han, M. Wang, K. L. Wang, R. B. Kaner, *Nano Lett.* **2007**, *7*, 3394.
[26] D. Li, M. B. Muller, S. Gilje, R. B. Kaner, G. G. Wallace, *Nat. Nanotechnol.* **2008**, *3*, 101.
[27] O. O. Van der Biest, L. J. Vandeperre, *Ann. Rev. Mater. Sci.* **1999**, *29*, 327.
[28] B. Gao, G. Z. Yue, Q. Qiu, Y. Cheng, H. Shimoda, L. Fleming, O. Zhou, *Adv. Mater.* **2001**, *13*, 1770.
[29] S. M. Jung, J. Hahn, H. Y. Jung, J. S. Suh, *Nano Lett.* **2006**, *6*, 1569.
[30] Z. S. Wu, W. Ren, L. Gao, C. Jiang, H. M. Cheng, *Carbon* **2009**, *47*, 493.
[31] A. R. Boccaccini, J. Cho, J. A. Roether, B. J. C. Thomas, E. J. Minay, M. S. P. Shaffer, *Carbon* **2006**, *44*, 3149.
[32] Y. B. Tang, H. T. Cong, Z. G. Zhao, H. M. Cheng, *Appl. Phys. Lett.* **2005**, *86*, 153104.
[33] I. Brodie, C. A. Spindt, *Adv. Electron. Electron. Phys.* **1992**, *83*, 1.
[34] K. Okano, S. Koizumi, S. R. P. Silva, G. A. J. Amaratunga, *Nature* **1996**, *381*, 140.
[35] M. C. Benjamin, C. Wang, R. F. Davis, R. J. Nemanich, *Appl. Phys. Lett.* **1994**, *64*, 3288.
[36] V. V. Zhirnov, G. J. Wojak, W. B. Choi, J. J. Cuomo, J. J. Hren, *J. Vac. Sci. Technol. A* **1997**, *15*, 1733.
[37] D. A. Lapianosmith, E. A. Eklund, F. J. Himpsel, L. J. Terminello, *Appl. Phys. Lett.* **1991**, *59*, 2174.
[38] J. D. Carey, S. R. P. Silva, *Solid-State Electr.* **2001**, *45*, 1017.
[39] X. Jiang, F. C. K. Au, S. T. Lee, *J. Appl. Phys.* **2002**, *92*, 2880.
[40] J. Hahn, S. M. Jung, H. Y. Jung, S. B. Heo, J. H. Shin, J. S. Suh, *Appl. Phys. Lett.* **2006**, *88*, 113101.
[41] W. Y. Sung, S. M. Lee, W. J. Kim, J. G. Ok, H. Y. Lee, Y. H. Kim, *Diam. Relat. Mater.* **2008**, *17*, 1003.
[42] D. S. Chung, W. B. Choi, J. H. Kang, H. Y. Kim, I. T. Han, Y. S. Park, Y. H. Lee, N. S. Lee, J. E. Jung, J. M. Kim, *J. Vac. Sci. Technol. B* **2000**, *18*, 1054.
[43] W. A. deHeer, J. M. Bonard, K. Fauth, A. Chatelain, L. Forro, D. Ugarte, *Adv. Mater.* **1997**, *9*, 87.
[44] B. Ha, D. H. Shin, J. Park, C. J. Lee, *J. Phys. Chem. C* **2008**, *112*, 430.
[45] K. Y. Chun, C. J. Lee, *J. Phys. Chem. C* **2008**, *112*, 4492.
[46] C. J. Lee, T. J. Lee, S. C. Lyu, Y. Zhang, H. Ruh, H. J. Lee, *Appl. Phys. Lett.* **2002**, *81*, 3648.
[47] T. Yu, Y. W. Zhu, X. J. Xu, Z. X. Shen, P. Chen, C. T. Lim, J. T. L. Thong, C. H. Sow, *Adv. Mater.* **2005**, *17*, 1595.
[48] H. J. Jeong, H. K. Choi, G. Y. Kim, Y. I. Song, Y. Tong, S. C. Lim, Y. H. Lee, *Carbon* **2006**, *44*, 2689.
[49] S. C. Lim, H. K. Choi, H. J. Jeong, Y. I. Song, G. Y. Kim, K. T. Jung, Y. H. Lee, *Carbon* **2006**, *44*, 2809.